



# W/HAP catalysed N-oxidation of tertiary amines with H<sub>2</sub>O<sub>2</sub> as an oxidant

RAKHI VISHWAKARMA, VIRENDRA RATHOD\* and  
LAKSHMI KANTAM MANNEPALLI\*

Department of Chemical Engineering, Institute of Chemical Technology, Nathalal Parekh Marg, Matunga, Mumbai 400019, India

E-mail: vk.rathod@ictmumbai.edu.in; lk.mannepalli@ictmumbai.edu.in

MS received 27 September 2021; revised 17 December 2021; accepted 28 January 2022

**Abstract.** Synthesis of several *N*-oxides with tungsten exchanged hydroxyapatite (W/HAP) in the presence of 30% hydrogen peroxide (H<sub>2</sub>O<sub>2</sub>) as an oxidant is presented. A process with aqueous H<sub>2</sub>O<sub>2</sub>, a cheap and clean oxidant with an active catalyst is developed to reduce waste production and meet the requirements of green chemistry. Several tertiary amines have been efficiently oxidized to their corresponding *N*-oxides with excellent yields. The as-synthesized catalyst (W/HAP) is characterized using BET, FTIR, SEM, ICP-OES and XRD. Effect of catalyst loading, temperature and oxidants were studied. A kinetic model has been developed to determine the reaction rate at different temperatures and activation energy for the model reaction.

**Keywords.** *N*-oxides; Tertiary amines; Hydroxyapatite; Green oxidants; Kinetic study.

## Abbreviations

A	Reactant species A, pyridine
B	Reactant species B, hydrogen peroxide
C	Product C, pyridine <i>N</i> -oxide
D	By-product D, water
C <sub>A</sub>	Concentration of A (mol/lit)
C <sub>B</sub>	Concentration of B (mol/lit)
-r <sub>A</sub>	Rate of surface reaction of A (mol lit s <sup>-1</sup> )
K	Second order rate constant (lit <sup>2</sup> . mol <sup>-1</sup> sec <sup>-1</sup> g <sup>-1</sup> )
W	Catalyst loading (g/lit)
C <sub>A0</sub>	Initial concentration of A, (mol/lit)
C <sub>B0</sub>	Initial concentration of B, (mol/lit)
X <sub>A</sub>	Fractional conversion of A
M	Initial molar ratio of reactants B to A

applications in the field of chemistry due to its various uses in organic and inorganic chemistry.<sup>1</sup> The oxidation of nitrogen compounds results in the synthesis of versatile building blocks for organic synthesis.<sup>2,3</sup> Table 1 provides an insight into different catalysts used for the oxidation of heterocyclic nitrogen compounds to their *N*-oxides using H<sub>2</sub>O<sub>2</sub> as an oxidant.

A greener catalytic oxidation method is one that utilizes dioxygen (O<sub>2</sub>) or hydrogen peroxide as an oxidant. Aqueous H<sub>2</sub>O<sub>2</sub> is an ideal oxidant because of its safety in storage and handling, high oxygen content, low production, and transportation cost, and is a green reagent that produces only water as a by-product.<sup>1</sup> Moreover, reactions performed in water are environmentally friendly. There is always a need to develop new processes to minimise the difference between atom utilization of actual and theoretical values for an increasingly global and environmental problem.<sup>6</sup>

Hydroxyapatite (HAP) [Ca<sub>10</sub>(PO<sub>4</sub>)<sub>6</sub>(OH)<sub>2</sub>] is a weak alkaline calcium phosphate. It has strong ion-exchange property, and it can be exchanged with the majority of metal ions. This property allows preparing the highly dispersed and stable metal-supported catalysts. The acidity and basicity on the surface of hydroxyapatite

## 1. Introduction

Pyridine is a six-membered heterocyclic nitrogen-containing compound. It occupies an important role in bioorganic and medicinal chemistry. Oxidation of pyridine to pyridine *n*-oxide has found novel

\*For correspondence

Supplementary Information: The online version contains supplementary material available at <https://doi.org/10.1007/s12039-022-02038-0>.

**Table 1.** Different types of catalysts used for N-Oxidation.

No.	Catalysts	Temperature (°C)	Time (h)	Yield (%)	Refs.
1	VS-1	60	12	90	4
2	TS-1	75	2	99	5
3	LDH-WO <sub>4</sub>	r.t.	3–5	96	6
4	Mg-Al-O-tBu hydrotalcite	75	1–5	98	7
5	Redox molecular sieves	60	5–24	90	8
6	V <sub>x</sub> Si <sub>4x</sub> O <sub>6.4x</sub>	80	3–12	45–99	9
7	Ru(PVP)/γ-Al <sub>2</sub> O <sub>3</sub>	r.t.	1–2	99	10
8	Poly(maleic anhydride-alt-1-octadecene)	90	7	93	11
9	MeReO <sub>3</sub>	r.t.	6	90	12
10	<i>m</i> -Chloroperbenzoic acid	r.t.	1–24	87	13
11	Na <sub>2</sub> WO <sub>4</sub> ·2H <sub>2</sub> O	– 5 and r.t.	3	40–89	14

can be changed by adjusting the calcium-phosphorus ratio. The surface of HAP is rich in hydroxyl groups, so it has strong absorbability and can be modified by organic compounds with polar functional groups and better support for organometallic compounds. HAP is used widely for the dehydrogenation of hydrocarbons, oxidation of alcohols, C-C bond formation reactions, and reduction reactions such as hydrogenolysis.<sup>15–20</sup> Choudary B M<sup>21</sup> reported three-component coupling to prepare propargylamine from aldehyde, alkyne, and an amine using copper-hydroxyapatite (CuHAP) under mild reaction parameters. Another work reported by Choudary B M<sup>22</sup> includes N-arylation of imidazoles and other heterocycles with fluoroarenes and chloroarenes using copper-exchanged *tert*-butoxyapatite and copper-exchanged fluorapatite. Kantam M L<sup>23</sup> synthesized *N*-arylimidazoles and *N*-arylamines at room temperature in the presence of copper fluorapatite (CuFAP). A palladium-supported fluorapatite catalyst (PdFAP) gave high activity for Suzuki coupling of bromides and aryl iodides with chloroarenes and boronic acids at 130°C and room temperature, respectively. The catalyst was also successful for Heck olefination of chloroarenes.<sup>24</sup> Hydrogenation of levulinic acid to  $\gamma$ -valerolactone was successfully obtained by metal (Ru, Pt, Pd, Ni) supported hydroxyapatites.<sup>16</sup> Kaneda K<sup>25</sup> discussed the active metal sites on the apatite compounds that display novel catalytic activity in selective oxidations, carbon-dioxide chemical fixation, carbon-carbon bond formation.<sup>22</sup> Their further review includes high-performance apatite-based catalysts for liquid-phase organic synthesis and continuous flow systems. Fihri A and Solhy A<sup>26</sup> highlighted the application of hydroxyapatite in heterogeneous catalysis and its synthesis methods with the structural properties.

Recently, there is a review article by Kantam M L<sup>27</sup> on C-C and C-N bond-forming reactions catalysed by HAP. There are various methods to synthesize hydroxyapatite. A stoichiometric HAP can be obtained from a balanced molar ratio of the calcium and phosphate precursors and maintaining pH.<sup>28</sup>

Pyridine *N*-oxides have wide applications as auxiliary agents, synthetic intermediates, oxidants, protecting groups, and as ligands in catalysts and metal complexes.<sup>11,29</sup> Ghaleb A<sup>30</sup> successfully studied the structure-activity relationship for a new family of SARS-CoV 3CL pro-inhibitors, pyridine *N*-oxide derivatives. Pyridine *N*-oxide compounds have antiviral activity against SARS. They reported pyridine *N*-oxide antiviral compounds to be more potent against SARS-CoV-2 than chloroquine and hydroxychloroquine.

Herein, we report the *N*-oxidation of tertiary amines to the corresponding *N*-oxides using H<sub>2</sub>O<sub>2</sub> as an oxidizing agent and tungsten exchanged hydroxyapatite (W/HAP) as a catalyst in water for three cycles at low temperature.

## 2. Experimental

### 2.1 Materials

All the chemicals were purchased from Oxford lab fine chem and used as received. The reaction progress was monitored by High performance liquid chromatography (Thermo Scientific, Ultimate 3000), Cosmosil C-18 column, 0.132 g of Sodium acetate buffer with 30% acetonitrile and 70% water, 0.6 mL/min of flow rate, 10 min total run time at the pressure of 65 bar. The surface area of the optimized catalyst was determined by Micromeritics ASAP 2000 instrument by

using Nitrogen adsorption-desorption isotherms. All the samples were degassed under vacuum for 4 h at 350 °C. ICP-OES is carried out by Agilent model: 5110. A Fourier Transform Infrared Spectrum (FTIR) of the catalysts was measured on a Perkin Elmer Spectrophotometer in the range of 400-4000  $\text{cm}^{-1}$ . Scanning electron microscopy (SEM) was obtained on Philips XL, 30 SEM, The Netherlands. XRD was obtained from Shimadzu X-ray diffractometer-6100 LabX.

## 2.2 Catalyst synthesis

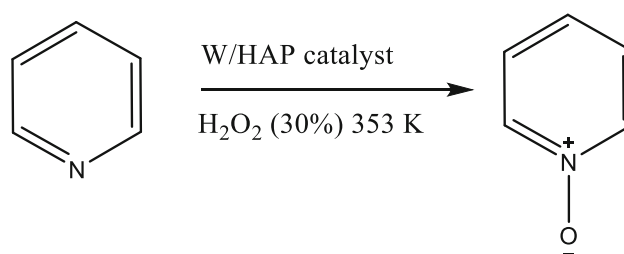
Hydroxyapatite was synthesized using the co-precipitation method.<sup>22</sup> 0.066 mol of calcium nitrate was dissolved in 60 mL of water, brought to 11-12 pH with concentrated ammonia solution and diluted to 120 mL. A solution of 0.04 mol of diammonium orthophosphate in 100 mL of water was prepared and brought to the pH of 11-12 using concentrated ammonia solution. The calcium solution was stirred at room temperature with the simultaneously addition of phosphate solution drop-wise over a period of 30 min and the milky solution was further stirred, boiled for 10 min at reflux. The precipitate was filtered, dried at 353 K overnight and calcined at 773 K for 3 h.

## 2.3 Tungstate exchanged hydroxyapatite

To 1 g of hydroxyapatite, 100 mL of sodium tungstate solution was added (1.87 mM, 0.616 g) and stirred at 293 K for 24 h. The catalysts were filtered off, washed, and dried at 353 K overnight.<sup>6,31,32</sup> The tungsten content in the W/HAP catalyst was found to be 0.0340 Wt.%.

## 2.4 Procedure for the N-Oxidation reaction

N-Oxidation of pyridine to pyridine N-Oxide was performed in a 50 mL glass reactor equipped with a 6-blade pitched turbine impeller. The reactor was immersed in an oil bath with PID controller to maintain the temperature of the oil bath. 2 mmol of pyridine was reacted with 6 mmol of 30% hydrogen peroxide ( $\text{H}_2\text{O}_2$ ) in the presence of W/HAP catalyst and 10 mL of water, 1200 rpm at 353 K for 20 h. The initial sample was collected when the reaction reached the desired temperature. Samples were taken out at fixed intervals up to 20 h and centrifuged to separate the catalyst particles. The reaction is depicted in Scheme 1.



**Scheme 1.** N-oxidation of Pyridine to Pyridine N-Oxide.

## 3. Results and Discussion

### 3.1 Catalysts characterization

The Brunauer-Emmett-Teller (BET) surface area of W/HAP was measured to be 91.4  $\text{m}^2/\text{g}$ , and the pore volume was 0.1318  $\text{cc}/\text{g}$ . The nitrogen adsorption-desorption isotherm for W/HAP is shown in (Figure S1, SI) was found to be type IV with the characteristic of mesoporous material having a small plateau at high relative pressure.

The FTIR spectra (Figure 1) of W/HAP displays  $\text{PO}_4$  vibrational frequencies in agreement with the literature,<sup>33,34</sup> bands were observed at 962  $\text{cm}^{-1}$ , for the symmetric P-O stretching  $\nu_1$ , at 1029 and 1060  $\text{cm}^{-1}$  for the asymmetric P-O stretching  $\nu_3$ . 450, 562, 602, 635, and 718  $\text{cm}^{-1}$  for the O-P-O bending modes  $\nu_2$  and  $\nu_4$ .

The SEM technique was used to investigate the size and shape of the synthesized material. The (Figure S2, SI) image (a) clearly indicates the particles are in the nanosize range. There are irregular agglomerates for the W/HAP sample from image (b) and literature.<sup>35</sup>

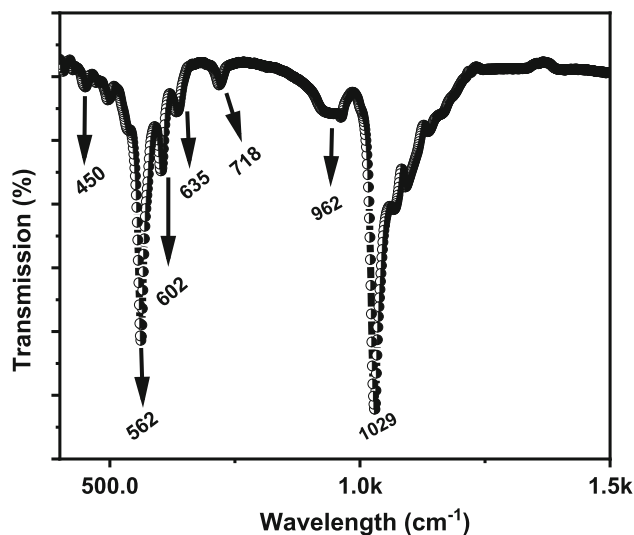


**Figure 1.** FTIR of W/HAP.

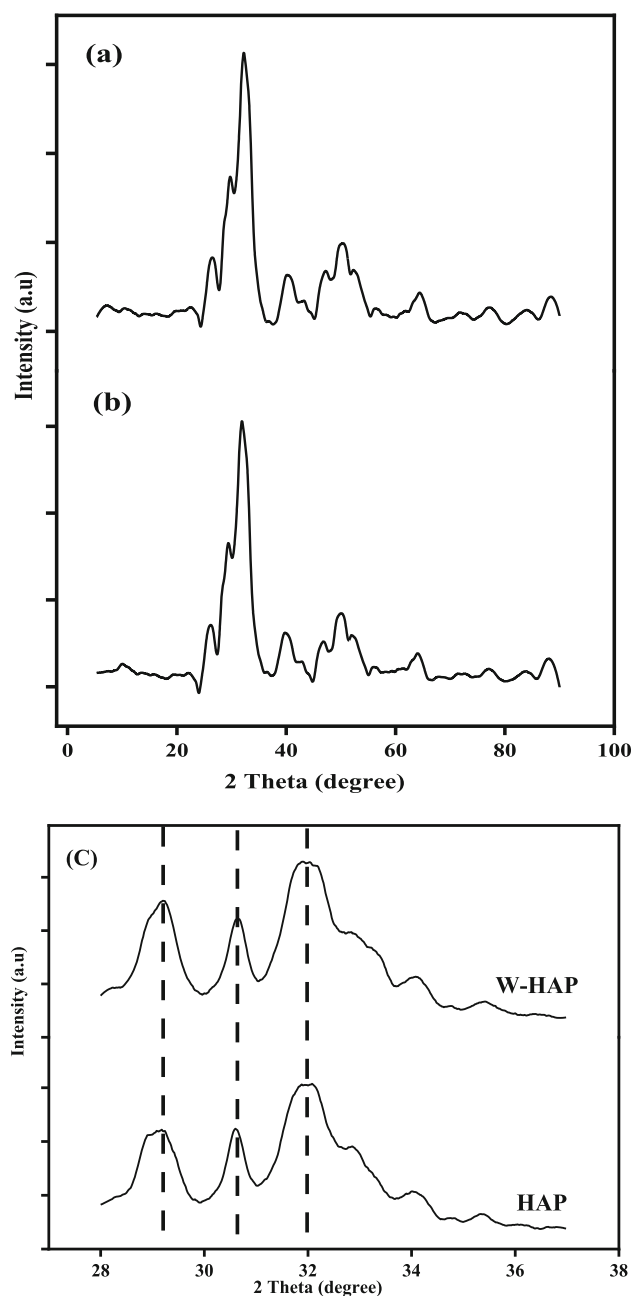


**Figure 2.** XRD of **a** HAP and **b** W/HAP **c** Inset of **a** and **b** showing detailed view.

These agglomerates consist of fine crystallites that are not visible individually because of their small size. The surface of the particles was found to be rough from image (c).

The XRD data of hydroxyapatite well matched with the reported JCPDS #09-0432. The XRD of W/HAP catalyst matches with the reported data (JCPDS# 11-0693). The crystallinity of the catalyst can be confirmed by the peaks reflection at 32° and 34° and planes corresponding are (300) and (112), respectively.<sup>34</sup> The other peaks are at the reflection of 25°, 26°, 29°, 30°, 38°, 40°, 41°, 46°, 49°, 50°, 51°, 53° are

in corresponding with (229), (105), (350), (300), (100), (99), (95), (105), (106), (98), (97), (101).

### 3.2 Catalytic activity

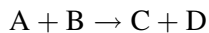
2 mmol of pyridine was reacted with 6 mmol of 30% hydrogen peroxide ( $\text{H}_2\text{O}_2$ ) in the presence of different catalysts and 10 mL of water at 353 K for 20 h. The conversion was 90 and 86%, respectively, with W/HAP and HAP. No by-products were formed in this reaction. The lowest conversion of 36% was found with FAP (Fluorapatite). Sodium tungstate and sodium molybdate afforded conversion of 70 and 75%, respectively. Whereas tungstate and molybdate loaded layered double hydroxides showed 58 and 44% conversion (Figure 3). A series of experiments were done using 5 wt% to 50 wt% of W/HAP catalyst, and 20 wt% catalyst gave 90% conversion (Figure 4). Catalyst loading was studied with respect to the limiting reactant. The optimization studies were conducted with 20 wt% of W/HAP catalyst (Figure 4).<sup>36</sup> The reaction was tested with different oxidants. 30%  $\text{H}_2\text{O}_2$  was found to be the best oxidant for the reaction with 90% conversion, and the conversion was less with the use of 70% aqueous TBHP and air, as shown in (Figure 5). The reaction was studied at varying molar ratios of pyridine to  $\text{H}_2\text{O}_2$  (Figure 6). We obtained an increase in yield with an increase in the amount of  $\text{H}_2\text{O}_2$ .<sup>4</sup> The speed of agitation was studied from 800 to 1200 rpm. There was a negligible difference in the rate of reaction and thus proves the absence of external mass transfer resistance in the reaction (Figure 7). Temperature study was carried out at 323, 333, 343, and 353 K. The highest conversion, 90%, was obtained at 353 K, and the lowest 60% at 323 K. Low conversion of 20% was obtained at room temperature, and water was found to be the best solvent for the reaction. Sample was analysed with time at all temperatures to determine the progress of the reaction as shown in (Figure 8). The TON and TOF are calculated as 5.05 and 0.25  $\text{h}^{-1}$ , respectively.

### 3.3 Substrate study

Substrates with structural diversity were studied at the optimized reaction conditions. We observed that all the aromatic nitrogen compounds were transformed into their corresponding *N*-Oxides, as shown in (Table 2).

### 3.4 Reaction mechanism and kinetic model

The reaction mechanism is presumed to be similar to that reported in the literature.<sup>6,37</sup>



A = Pyridine, B = H<sub>2</sub>O<sub>2</sub>, C = Pyridine N-Oxide, D = Water

$$-r_A = \frac{-dC_A}{dt} = \frac{-dC_B}{dt} = K C_A C_B W$$

$$\begin{aligned} -r_A &= C_{A0} \frac{dX_A}{dt} \\ &= K(C_{A0} - C_{A0} \cdot X_A)(C_{B0} - C_{A0} \cdot X_A) \end{aligned}$$

Let  $M = \frac{C_{B0}}{C_{A0}}$  be the initial molar ratio of reactants, we obtain

$$-r_A = C_{A0} \frac{dX_A}{dt} = K C_{A0}^2 (1 - X_A)(M - X_A)$$

Integrating the above equation, we get

$$\int_{C_{A0}}^{C_A} \frac{dX_A}{(1 - X_A)(M - X_A)} = K C_{A0} W \int_0^t dt$$

$$\ln \frac{M - X_A}{M(1 - X_A)} = K C_{A0} (M - 1) W t \quad (1)$$

Plotting the above equation as a graph with the slope as  $K C_{A0} (M - 1) W$ ,

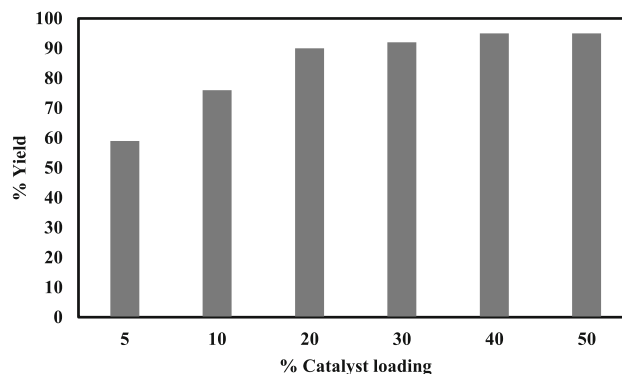


**Figure 4.** Effect of catalyst loading on yield of pyridine N-oxide. Reaction conditions: Pyridine: 2 mmol, oxidant: 6 mmol, W/HAP, 10 mL water, 1200 rpm, 353 K, 20 h.

Graph of  $\ln \frac{M - X_A}{M(1 - X_A)}$  V/s Time:

The experimental data were used to verify the validity of the equation (1) and plotted as shown in (Figure 9). Using equation (1), plots were made for different temperatures with respect to time, and the rate constants were calculated mentioned in (Table 3). These rate constants were used for the calculation of activation energy by plotting an Arrhenius plot (Figure 10) as 50 Kcal/mol, which supports the fact that the N-oxidation of pyridine was kinetically controlled.

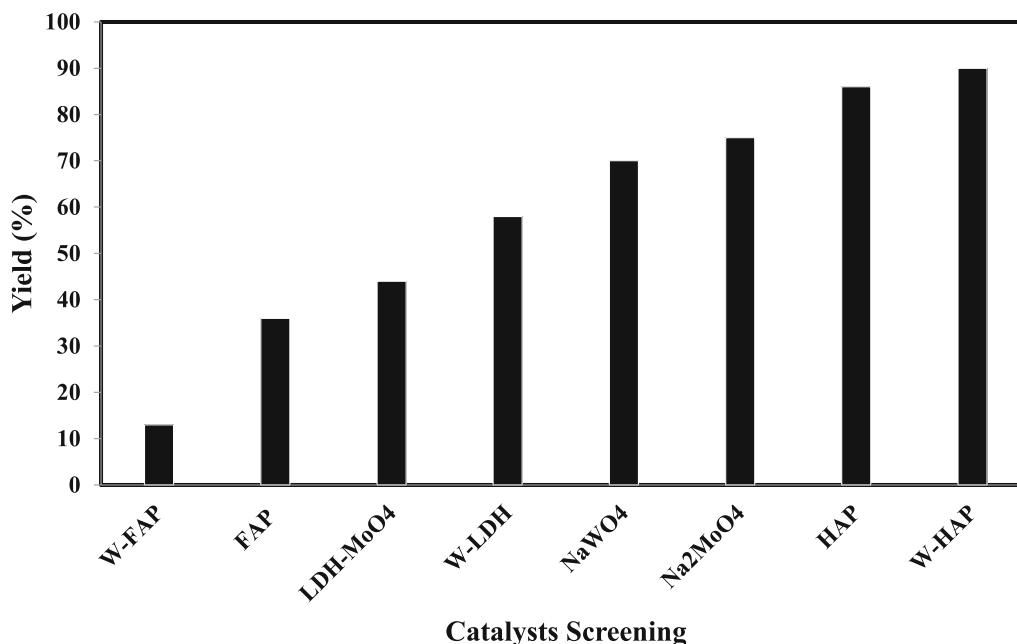


**Figure 3.** Effect of different catalysts on the yield of Pyridine N-oxide. Reaction conditions: Pyridine: 2 mmol, H<sub>2</sub>O<sub>2</sub>: 6 mmol, catalyst: 200 mg, 10 mL water, 1200 rpm, 353 K, 20 h.

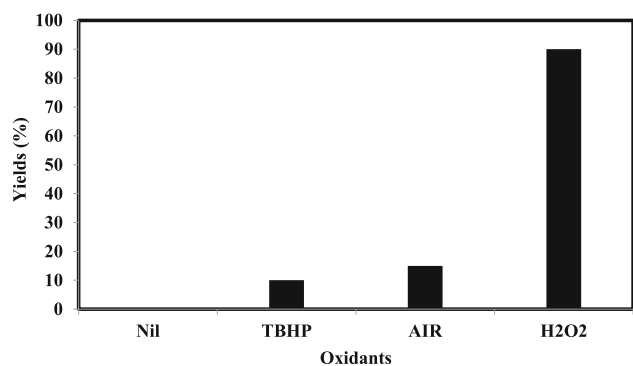


**Figure 5.** Effect of different oxidants on the yield of Pyridine N-Oxide. Reaction conditions: Pyridine: 2 mmol, oxidant: 6 mmol, 20% W/HAP, 10 mL water, 1200 rpm, 353 K, 20 h.

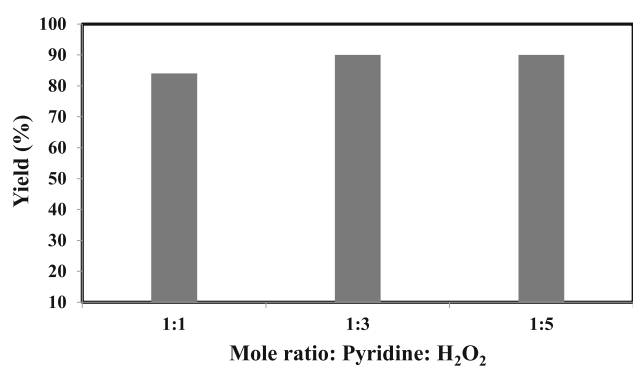


**Figure 6.** Effect of mole ratio on the yield of Pyridine N-Oxide. Reaction conditions: Pyridine: 2 mmol, 20% W/HAP, 10 mL water, 1200 rpm, 353 K, 20 h.

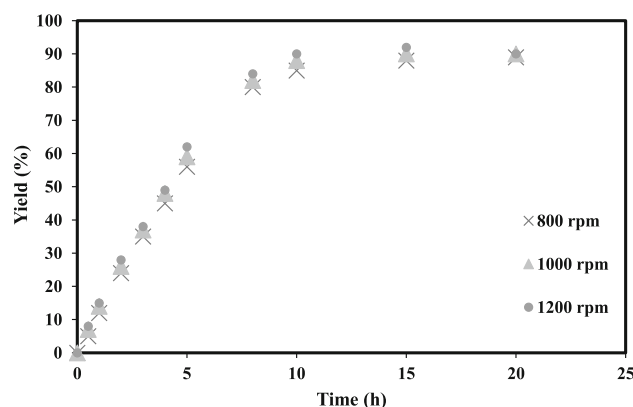


**Figure 7.** Effect of speed of agitation on the yield of Pyridine N-Oxide. Reaction conditions: Pyridine: 2 mmol, oxidant: 6 mmol, 20% W/HAP, 10 mL water, 353 K, 20 h.

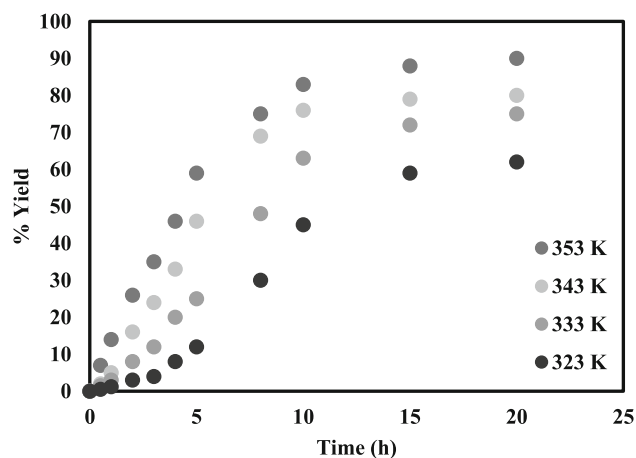


**Figure 8.** Effect of temperature on the yield of Pyridine N-oxide. Reaction conditions: Pyridine: 2 mmol, H<sub>2</sub>O<sub>2</sub>: 6 mmol, 20% W/HAP, 10 mL water, 1200 rpm, 20 h.

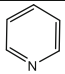
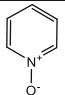
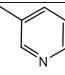
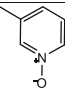
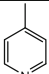
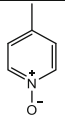
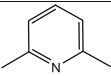
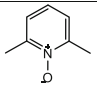
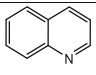
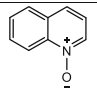
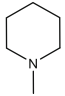
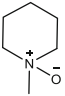
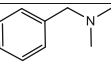
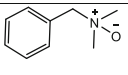
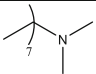
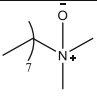
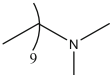
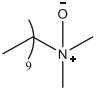
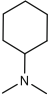
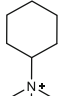
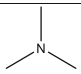
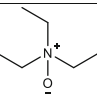
### 3.5 Reusability of catalyst

The reusability of catalysts was studied. The catalyst was separated by centrifuging the reaction mixture after the reaction. The catalyst separated was refluxed in water for 5 h to remove the adsorbed materials from the catalyst surface and dried at 373 K overnight. There was no loss of catalyst during the separation process. The catalyst was used three times. During the third use, we observed a slight decrease in conversion. The leaching experiments were also performed after each cycle, and the amount of tungsten was determined after each cycle. There was marginal leaching of tungsten after each cycle. This must be the reason for a slight decrease in the performance of the catalyst (Figure 11).

## 4. Conclusions

A simple and efficient procedure is developed for the synthesis of *N*-oxides using eco-friendly H<sub>2</sub>O<sub>2</sub> as an oxidant and reusable W/HAP catalyst. Several catalysts were studied among which W/HAP was found to be the best catalyst among all the screened catalysts. The as-prepared and optimized catalyst was characterized by various analytical techniques such as N<sub>2</sub> adsorption-desorption, SEM, XRD, ICP-OES and

**Table 2.** N-Oxidation of various tertiary amines in the corresponding N-Oxide.

Sr. No	Substrate	Product	Yield (%)
1			90 <sup>a</sup>
2			89 <sup>a</sup>
3			47 <sup>a</sup>
4			69 <sup>a</sup>
5			20 <sup>a</sup>
6			94 <sup>b</sup>
7			92 <sup>b</sup>
8			89 <sup>b</sup>
9			94 <sup>b</sup>
10			92 <sup>b</sup>
11			91 <sup>b</sup>

Reaction conditions: Pyridine: 2 mmol, H<sub>2</sub>O<sub>2</sub>: 6mmol, 10 mL water, 1200 rpm, 353 K, 20% W/HAP, 20 h

<sup>a</sup>Substrates analysed by HPLC

<sup>b</sup>Substrates analysed by GC



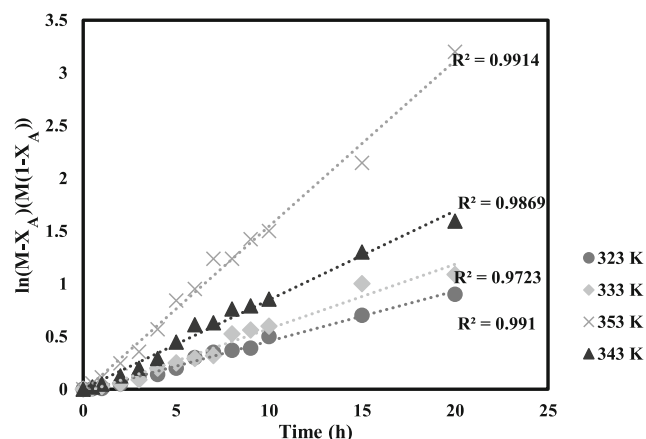


**Figure 9.** Plot of  $\ln(M-X_A)(M(1-X_A))$  Vs Time.

**Table 3.** Rate constants at different reaction temperature.

Temperature (K)	(K) $\text{lit}^2 \cdot \text{mol}^{-1} \text{sec}^{-1} \text{g}^{-1}$
323	0.00686
333	0.009440
343	0.01326
353	0.03709

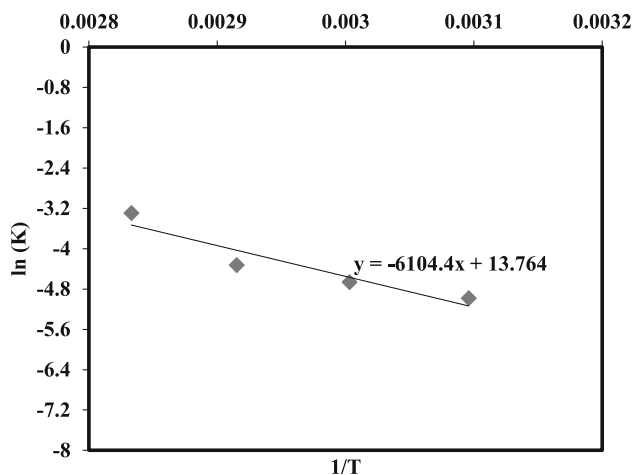


**Figure 10.** Activation energy by Arrhenius plot.

FTIR. A broad substrate study was done and a kinetic study was also carried out.

### Supplementary Information (SI)

Supplementary Information contains the nitrogen adsorption-desorption isotherm and SEM images of W/HAP catalyst, LCMS and GCMS data of products. Supplementary information is available at [www.ias.ac.in/chemsci](http://www.ias.ac.in/chemsci).

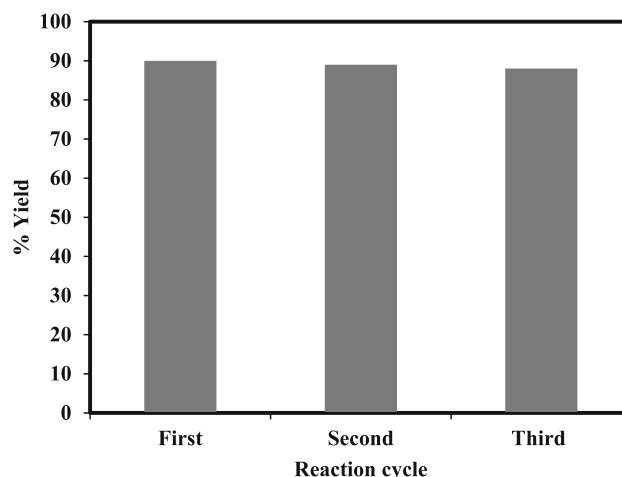


**Figure 11.** Catalyst Reusability study. Reaction conditions: Pyridine: 2 mmol,  $\text{H}_2\text{O}_2$ : 6 mmol, 10 mL water, 353 K, 1200 rpm, 20% W/HAP, 20 h.

### Acknowledgements

MLK acknowledges support from Godrej Consumer Products Limited (GPCL) for Dr. B. P. Godrej Distinguished Chair Professor and J.C. Bose National Fellowship (SERB-DST, GoI). Rakhi acknowledges the funding support by Godavari Biorefineries Ltd. and FICCI-SERB for Prime Minister's Fellowship Scheme for Doctoral Research.

### References

1. Veerakumar P, Balakumar S and Velayudham M 2012 Ru/ $\text{Al}_2\text{O}_3$  catalyzed N-oxidation of tertiary amines by using  $\text{H}_2\text{O}_2$  *Catal Sci. Technol.* **2** 1140
2. Thiel W R 2003 Transition metal mediated oxygen transfer to organo nitrogen compounds *Coord. Chem. Rev.* **245** 95
3. Campeau L, Stuart D R, Leclerc J, Villemure E, Sun H, Lasserre S, et al. 2009 Palladium-catalyzed direct arylation of azine and azole N-oxides: reaction development, scope and applications in synthesis *J. Am. Chem. Soc.* **131** 3291
4. Phukan P, Khisti R S and Sudalai A 2006 Green protocol for the synthesis of N-oxides from secondary amines using vanadium silicate molecular sieve catalyst *J. Mol. Catal. A Chem.* **248** 109
5. Xie W, Zheng Y, Zhao S, Yang J, Liu Y and Wu P 2010 Selective oxidation of pyridine- N -oxide with hydrogen peroxide over Ti-MWW catalyst *Catal. Today* **157** 114
6. Choudary B M, Bharathi B, Reddy C V and Kantam M L 2002 The first example of heterogeneous oxidation of secondary amines by tungstate-exchanged Mg-Al layered double hydroxides: a green protocol *Green Chem.* **4** 279
7. Choudary B M, Reddy CV, Prakash B V, Bharathi B and Kantam M L 2004 Oxidation of secondary and



- tertiary amines by a solid base catalyst *J. Mol. Catal. A Chem.* **217** 81
8. Ramakrishna Prasad M, Kamalakar G, Madhavi G, Kulkarni S J and Raghavan K V 2002 An efficient synthesis of heterocyclic N-oxides over molecular sieve catalysts *J. Mol. Catal. A Chem.* **186** 109
  9. Rout L and Punniyamurthy T 2005 Silica-supported vanadium-catalyzed n -oxidation of tertiary amines with aqueous hydrogen peroxide *Adv. Synth. Catal.* **347** 1958
  10. Veerakumar P, Lu Z, Velayudham M, Lu K and Rajagopal S 2010 Alumina supported nanoruthenium as efficient heterogeneous catalyst for the selective H<sub>2</sub>O<sub>2</sub> oxidation of aliphatic and aromatic sulfides to sulfoxide *J. Mol. Catal. A Chem.* **332** 128
  11. Gajeles G, Kim S M, Yoo J C, Lee K K and Lee S H 2020 Recyclable anhydride catalyst for H<sub>2</sub>O<sub>2</sub> oxidation: N-oxidation of pyridine derivatives *RSC Adv.* **10** 9165
  12. Copéret C, Adolffson H, Khuong TV, Yudin A K and Sharpless K B A 1998 Simple and efficient method for the preparation of pyridine N -oxides *J. Org. Chem.* **3263** 1740
  13. Tokuyama H, Kuboyama T and Fukuyama T 2003 Transformation of primary amines to N-monoalkylhydroxylamines: N-hydroxy-(S)-1-phenylethylamine oxalate *Org. Synth.* **80** 207
  14. Murahashi S, Shiota T and Imada Y 1992 Oxidation of secondary amines to nitrones: 6-methyl-2,3,4,5-tetrahydropyridine N-oxide *Org. Synth.* **70** 265
  15. Boukha Z, Ayastuy J L, Cortés-Reyes M, Alemany L J, González-Velasco J R and Gutiérrez-Ortiz M A 2019 Catalytic performance of Cu/hydroxyapatite catalysts in CO preferential oxidation in H<sub>2</sub> -rich stream *Int. J. Hydrogen Energy* **44** 12649
  16. Sudhakar M, Kantam M L, Jaya S V, Kishore R, Ramanujacharya K V and Venugopal A 2014 Hydroxyapatite as a novel support for Ru in the hydrogenation of levulinic acid to  $\gamma$ -valerolactone *Catal. Commun.* **50** 101
  17. Moteki T and Flaherty D W 2016 Mechanistic insight to C-C bond formation and predictive models for cascade reactions among alcohols on Ca- and Sr-hydroxyapatites *ACS Catal.* **6** 4170
  18. Kaneda K and Mizugaki T 2017 Design of high-performance heterogeneous catalysts using apatite compounds for liquid-phase organic syntheses *ACS Catal.* **7** 920
  19. Guo J, Yu H, Dong F, Zhu B, Huang W and Zhang S 2017 High efficiency and stability of Au-Cu/hydroxyapatite catalyst for the oxidation of carbon monoxide *RSC Adv.* **7** 45420
  20. Mori K, Hara T, Mizugaki T, Ebitani K and Kaneda K 2004 Hydroxyapatite-supported palladium nanoclusters: A highly active heterogeneous catalyst for selective oxidation of alcohols by use of molecular oxygen *J. Am. Chem. Soc.* **126** 10657
  21. Choudary B M, Sridhar C, Kantam M L and Sreedhar B 2004 Hydroxyapatite supported copper catalyst for effective three-coupling reaction *Tetrahedron Lett.* **45** 7319
  22. Choudary B M, Sridhar C, Kantam M L, Venkanna G T and Sreedhar B 2005 Design and evolution of copper apatite catalyst for N-arylation of heterocycles with chloro- and fluoro arenes *J. Am. Chem. Soc.* **127** 9948
  23. Kantam M L, Venkanna G T, Sridhar C, Sreedhar B and Choudary B M 2006 An efficient base-free N-arylation of imidazoles and amines with arylboronic acids using copper-exchanged fluorapatite *J. Org. Chem.* **71** 9522
  24. Kantam M L, Kumar K B S, Srinivas P and Sreedhar B 2007 Fluorapatite-supported palladium catalyst for suzuki and heck coupling reactions of haloarenes *Adv. Synth. Catal.* **349** 1141
  25. Kaneda K and Mizugaki T 2009 Development of concerto metal catalysts using apatite compounds for green organic syntheses *Energy Environ. Sci.* **2** 655
  26. Fihri A, Len C, Varma R S and Solhy A 2017 Hydroxyapatite: A review of syntheses, structure and applications in heterogeneous catalysis *Coord. Chem. Rev.* **347** 48
  27. Gadipelly C, Deshmukh G and Kantam M L 2021 Transition metal exchanged hydroxyapatite/fluorapatite catalysts for C–C and C–N bond forming reactions *Chem. Rec.* **21** 1398
  28. Mohd Pu'ad N A S, Abdul Haq R H, Mohd Noh H, Abdullah H Z, Idris M I and Lee T C, 2019 Synthesis method of hydroxyapatite: A review *Mater. Today Proc.* **29** 233
  29. Malkov A V, Bell M, Castelluzzo F and Kočovský P 2005 METHOX: A new pyridine N-oxide organocatalyst for the asymmetric allylation of aldehydes with allyltrichlorosilanes *Org. Lett.* **7** 3219
  30. Ghaleb A, Aouidate A, El Ayouchia H B, Aarjane M, Anane H and Stiriba S E 2020 In silico molecular investigations of pyridine N-Oxide compounds as potential inhibitors of SARS-CoV-2: 3D QSAR, molecular docking modeling, and ADMET screening *Biomol. Struct. Dyn.* **40** 1
  31. Mekrattanachai P, Cao C, Li Z, Li H and Song W 2018 Cobalt immobilized on hydroxyapatite as a low-cost and highly effective heterogeneous catalyst for alkenes epoxidation under mild conditions *RSC Adv.* **8** 37303
  32. Sels B, Vos D D, Buntinx M, Peirard F, Mesmaeker A K D and Jacobs P 1999 Layered double hydroxides exchanged with tungstate as biomimetic catalysts for mild oxidative bromination *Nature* **400** 855
  33. Wuyts S, De Vos D E, Verpoort F, Depla D, De Gryse R and Jacobs P A 2003 A heterogeneous Ru-hydroxyapatite catalyst for mild racemization of alcohols *J. Catal.* **219** 417
  34. Ślósarczyk A, Paszkiewicz Z and Paluszkiwicz C 2005 FTIR and XRD evaluation of carbonated hydroxyapatite powders synthesized by wet methods *J. Mol. Struct.* **744–747** 657
  35. Shkir M, Kilany M and Yahia I S 2017 Facile microwave-assisted synthesis of tungsten-doped hydroxyapatite nanorods: A systematic structural, morphological, dielectric, radiation and microbial activity studies *Ceram. Int.* **43** 14923
  36. Gupta S S R, Vinu A and Kantam M L 2020 Copper-catalyzed oxidative methyl-esterification of

- 5-hydroxymethylfurfural using TBHP as an oxidizing and methylating reagent: A new approach for the synthesis of furan-2,5-dimethylcarboxylate *J. Catal.* **389** 259
37. Li Q, Luo W, Lu W and Wang Z 2016 Heterogeneous catalytic oxidation of pyridines to N-oxides under mild conditions using *React. Kinet. Mech. Catal.* **119** 235